U.P.B. Sci. Bull., Series A, Vol. 82, Iss. 3, 2020 ISSN 1223-7027

TESTING AND VERIFICATION METHODS FOR DIELECTRIC MIRRORS USED IN FEMTOSECOND REGIME LASER SYSTEMS

Ionela GHITA[1], Adrian RIZEA[2], Marian ZAMFIRESCU[3], Daniel OANCEA[4] Andrei NAZIRU[5], Mugurel GEORGESCU[6], Amélie LACHAPELLE[7], Gabriel COJOCARU[8], Razvan UNGUREANU[9], Costel COTIRLAN-SIMIONIUC[10]

This paper presents the methodology and reports the results concerning the Laser Induced Damage Threshold (LIDT), surface quality and group delay dispersion (GDD) measurements of large aperture femtosecond laser mirrors, achieved in a project funded by IFA under the contract number 02 ELI/18.10.20.17., having, as a main goal, the manufacturing of large aperture mirrors (150mm effective diameter) and tests performing for use in high energy ultra-short pulse laser systems, such as ELI-NP and CETAL infrastructures. The manufacturing process of the mirror substrates was described in a previous paper [1] and the coating technology will be presented in a future article. The novelty of this paper consists, mainly, in the method, experimental arrangement and test procedure to determine the Laser Induced Damage Threshold (LIDT) but also in the entire testing protocol, including Group Delay Dispersion (GDD) and other measurements presented here.

Keywords: laser mirrors, laser induced damage threshold, optical measurements.

1. Introduction

In the recent years, a great deal of interest was manifested towards laser systems which can deliver short pulses with high intensities, in particular on their interaction with matter, including the state of plasma [2]. Modern laser technology is pushed to its limits by the new concepts and state-of-the-art applications in order to obtain high-energy laser pulses with ultra-short duration [2]. The peak power handling capability of ultrashort pulse lasers is the main concern for new scientific facilities, like the "Extreme Light Infrastructure" (ELI). The

[1] [1] Eng.-corresponding author, Pro Optica, Romania, e-mail: ionela.ghita@prooptica.ro
[2] PhD., Pro Optica, Romania, e-mail: adrian.rizea@prooptica.ro
[3] PhD., INFLPR, Romania, e-mail: marian.zamfirescu@inflpr.ro
[4] PhD., Pro Optica, Romania, e-mail: daniel.oancea@prooptica.ro
[5] Eng., ELI-NP, Romania, e-mail: andrei.naziru@eli-np.ro
[6] Phys., Pro Optica, Romania, e-mail: mugurel.georgescu@prooptica.ro
[7] Phys., ELI-NP, Romania, e-mail: amélie.lachapelle@eli-np.ro
[8] Phys., INFLPR, Romania, e-mail: gabriel.cojocaru@inflpr.ro
[9] Phys., INFLPR, Romania, e-mail: razvan.ungureanu@inflpr.ro
[10] PhD., NIMP, Romania, e-mail: cotirlan@infim.ro

amplification of short pulses to high energies is limited by constraints of size and damage threshold of the optical components in the laser system due to the nonlinear optical effects that might appear with a large irradiance value.

Another aspect of interest with respect to the manufacturing of large aperture coated mirrors is the possibility of obtaining chirped mirrors, which could have a large impact in the development of post-compression of ultrashort laser pulses, thus increasing even further the peak power of laser systems based on Chirped Pulse Amplification technology.

A complete technological chain for manufacturing and testing large aperture dielectric mirrors is required. The challenge of this approach being the production itself of this kind of optical components, due to the large aperture and high surface quality requirements and the measurement method for determining the laser induced damage threshold. In order to safely use an optical component, the energy fluence has to be roughly 5 times lower than the damage value, i.e. in the ELI case, around 0.2 J/cm^2 [2]. This will correspond to a mirror surface of 500 cm^2, or 260-mm size optics. For 10-fs, 300-J pulses, optics of 450 mm size will be needed. The state-of-the-art 1” dispersive optics has a damage threshold of 0.1–0.2 J/cm^2 for 30–150fs pulses.

The interest for the effect of femtosecond laser pulses on matter started from the 50s of the last century by M.I. Kaganov, I. M. Lifshitz, L.V. Tanatarov. They described a mathematical model of the non-equilibrum heating of the condensed medium by the action of short and ultra-short-range pulse laser radiation [3]. Damage produced by short pulses in the femtosecond range is more confined than with longer pulses. Short pulses require less energy than longer pulses to reach the intensity necessary to produce optical breakdown. Less energy deposition leads to more precise ablation or material modification [4].

The major drawback in such kind of systems being the optical components, in particular mirrors, which get easily damaged during the operation due to the high intensities. In this context, we propose a methodology and report the results concerning the LIDT, surface quality and GDD measurements of a set of large aperture femtosecond laser mirrors.

In this context, a specific protocol and methods for characterization of optical components, used for transporting and focuses of the laser beam, appeared as one of the main priorities. Since a part of tests and measurements can be done on the witness plates (such as: roughness, spectral reflectance, laser induced damage threshold (LIDT) and group delay dispersion (GDD)), other measurements can be done only on the functional part (flatness or deviation from the desired shape of the surfaces, effective aperture, defects on the active surface, cleanliness, root-mean-square wavefront error (RMS).

2. Description of the methods

A femtosecond laser is a laser which generates ultrashort optical pulses with a duration in the femtoseconds domain. Ultrashort laser systems have the capacity to deliver to the desired target high amounts of power per pulse, thus being relevant in studying the behavior of matter in highly excited states but the frequent damage of the optics used for laser beam transport and focus, results in a high costs and long periods of maintenance. Laser mirrors should be able to withstand high power pulses and should have high optical quality (reflectivity, flatness and roughness). To have the complete description and specifications of the final mirrors that will be practically used in the daily analysis, a series of tests have to be applied both on the fabrication flux and to the completed mirrors. Each important parameter of the high-power laser mirror can be tested by several methods. In this paper we describe the most advantageous methods that we consider to be optimal for the inspection and analysis. Even if the methods presented have a general applicability, the results describe the performances of a mirror designed and fabricated by the authors, having the following main characteristics: **Overall diameter**: 156mm; **Effective diameter**: 150mm; **Thickness**: 50mm; **Coating**: 24 layers in a specific formula of HfO_2 – SiO_2.

Table 1

Proposed measurements

No.	**Measurements required by the uncoated substrate**	**Method used for the measurement**
1	Flatness and Root-mean-square wavefront error (RMS)	Phase Shifting Interferometry (measurement done on the 156 mm diameter substrate, before and after coating)
2	Roughness	Optical profilometry (AFM) (measurement done on witness plates, before and after coating)
3	Spectral reflectance	Spectrophotometry (measurement done on witness plates)
4	Laser Induced Damage Threshold (LIDT)	LIDT testing method (measurement done on witness plates)
5	Group Delay Dispersion (GDD)	White Light Interferometer (measurement done on witness plates)

2.1. **Flatness and Root-mean-square wave front error (RMS)** measurements can be very accurate performed by the Phase Shifting Interferometry. The drawback of this method is the aperture limitation (classical phase shifting interferometry have an aperture between 100 mm and 150 mm).

The principle of interferometric contouring relies on the optical comparison between an optical part under test and a plane or spherical reference surface of well-known surface accuracy. In order to achieve the necessary accuracy in the sub-micron range, the wavelength of the Helium/Neon-Laser of 632,8 nm is used to generate the interference pattern.

The results for the uncoated substrate (Figure 1a), and for the final mirror, coated and assembled in its frame (Figure 1b) are described in table 2.

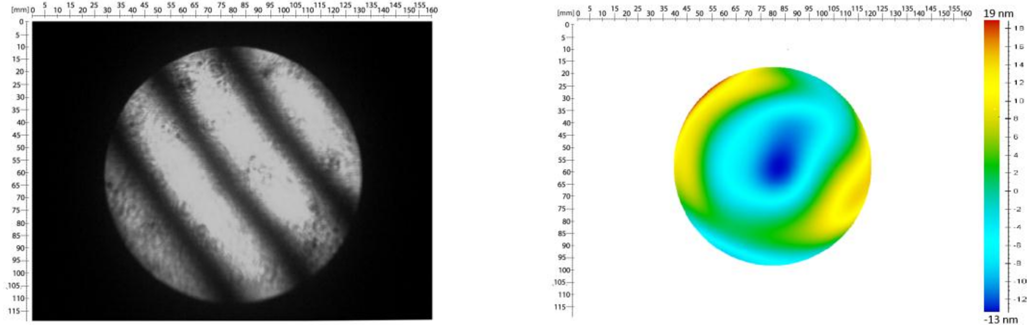

Fig.1. a. Interference figure expressing the flatness for the polished substrate

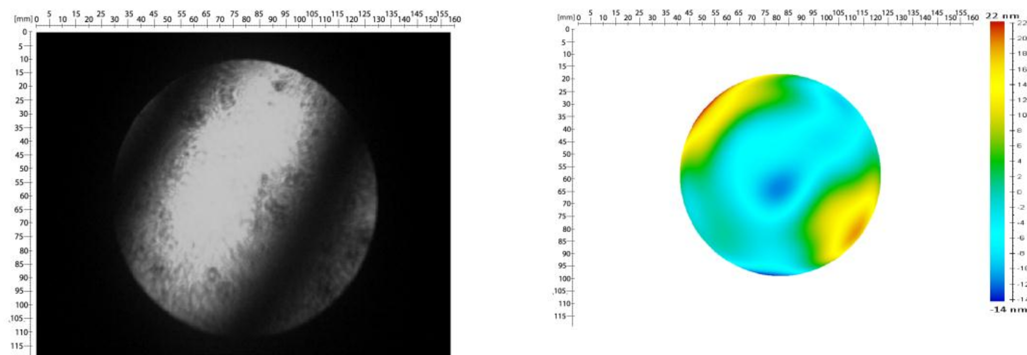

Fig.1. b. Interference figure expressing the flatness for the coated and assembled mirror

Table 2

The results for the uncoated substrate and for the final mirror

Property	Piece no.1 (The polished substrate)	Piece no.2 (The final mirror)
Peak-to-valley	32 nm	37 nm
RMS	7 nm	7 nm
Measured area	159.44 mm x 119.58 mm	159.44 mm x 119.58 mm

2.2. **Roughness:** Testing the roughness of the high-power laser mirrors could be performed by different methods, such as: Optical profilometry, Light and x-ray scattering and Scanning Probe Microscopy. Even though the optimal choice for high precision roughness measurements is the Scanning Probe Microscopy, with the main advantage of the high-resolution measurement with a lateral resolution limit of around one angstrom, we chose the Optical Profilometry and

for the coated samples because it has the advantage to be a fast, non-contact method with a sub-nanometer height resolution. The second method chosen for determining the roughness of the coated samples was Atomic Force Microscopy. The roughness of the samples was determined using the interferometric method because it is best suited for measuring the surface characteristics of well-polished continuous structures, having a sub nanometer vertical resolution. The topography of the measured surface is generated using the interference pattern obtained between a reference optical flat and the measured probe, in a similar way as the flatness measurement.

The key component in the structure of the profilometer is the Mirau type objective. The objective scans a 300 µm 2 surface of the measured sample and delivers the interference pattern to a CCD camera.

Based on the information obtained from the interference pattern, the profilometer software computes the arithmetic mean deviation of the surface, the standard deviation of the height distribution of the surface and other parameters as well, like the maximum peak height, the height between the highest peak and the deepest valley etc.

$$S_q = \sqrt{\frac{1}{A}\iint_A z^2(x,y)\,dxdy} \tag{1}$$

Sq – Root-mean-square height
A – Surface area

$$S_a = \sqrt{\frac{1}{A}\int_A |z(x,y)|\,dxdy} \tag{2}$$

Sa -Arithmetical mean height

Another well suited measuring technique for determining the roughness both of the coated and uncoated samples is Atomic Force Microscopy (AFM). This type of measurement procedure was chosen because of the fraction of nanometer accuracy and the advantage of not damaging the sample in any way.

For imaging the roughness topography of the coated sample, alternative contact or “tapping-mode” was used. When the measurement starts, the cantilever with oscillates at a slightly smaller frequency than its resonant frequency, which is 279 kHz, just above the surface of the measured sample. The cantilever’s probe tip is tapping the surface of the sample. While the sample changes its position, the oscillation amplitude modifies along with the change in roughness height. The feedback circuit closes the height feedback loop and makes the distance between the probe tip and the surface as small as possible. The changes in amplitude are monitored and the vertical displacement is measured using a laser beam that reflects from the cantilever into a photodiode [7].

The “tapping mode” measurement provides some advantages compared with the “contact mode” or “non-contact mode” measurement methods. It

eliminates the lateral forces with a high efficiency, it has a high lateral resolution on most samples and the probe tips and the examined samples are less likely to get damaged because the forces applied on it are considerably reduced [8].

Samples fabricated under the project were measured by AFM, using the above described method and the results were an average of less than 2 nm RMS as it can be seen in figure 2. Measuring system: AFM; Scanning mode: alternative contact; Resonance frequency of the cantilever: 279 kHz; RMS= 1.24 nm

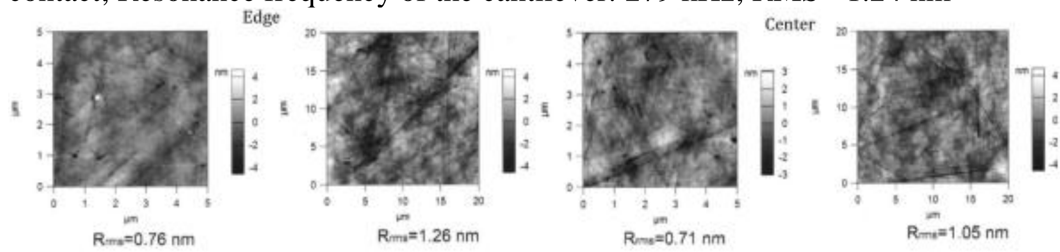

Fig. 2 Results obtained using AFM method for surface roughness of the test witnesses

2.3. **Spectral reflectance** is a measurement that can be easily done using a spectrophotometer. As it is well known, the beam of the femtosecond lasers has around of 50nm large spectral band and the mirror must cover this band at the designed angle of incidence. The mirrors fabricated were designed for an incidence angle of 45 deg. The measurement can be done in two ways: directly, measuring the reflection, but in this case a very high accurate reflection reference accessory is needed, mostly being used a non-protected silver coated plate. The disadvantage of this method consists in the fact that the silver layer decay very rapidly after manufacturing and, as a consequence, the reflection reference will never be trusted. The second way is to measure the complementary transmission, this being the method that was chosen, approximating the total loses by absorption to be quasi-zero. Transmissions of some witness plates at an incidence of 45 deg. are shown in figure 3.

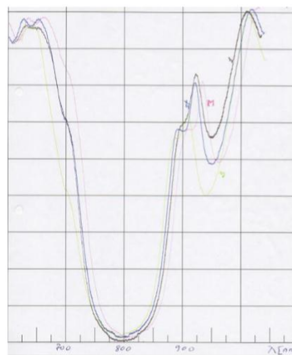

Fig.3 Transmissions of some witness plates at an incidence of 45 deg

Noting a transmission less than 2% in the interval [775, 825] nm, the resulted reflection can be deducted to be higher than 98%.

2.4. **Laser Induced Damage Threshold** is a particularly relevant measurement for optical elements, such as mirrors and gratings, designed to work in a laser system. The LIDT measurement depends on many parameters of the laser beam and for ultrashort laser pulses there are various theories describing the mechanism behind it. Some of the proposed damage processes are coulomb explosion [9], thermal melting [10], plasma formation [10] and material cracking caused by thermo-elastic stress. Even though the physical processes which describe the damage induced by the ultrashort pulses are different, all of them manifest at a certain critical value of the energy density.

The most used technique for the LIDT characterization of the dielectric mirrors is the S-on-1 test. The S-on-1 test consists in exposing the measured sample, which is divided into a matrix of sites or regions with known surface area to a pulsed laser beam of constant fluency. The number of pulses used to determine the damage threshold can vary from one application to another. In this particular case, the working regime consisted of using a single pulse or a train of two to ten pulses per site, with a 10 Hz repetition rate. After one site is tested, the fluency is increased and the procedure is repeated on the next region. If there is any sign of damage on the tested optical surface, the laser exposure is stopped. The number of pulses which landed on the tested site before the appearance of any damage is recorded and counted. Based on this number, the LIDT value is determined. The final result is expressed as a probability of damage occurrence with respect to the number of incident pulses.[11]

An experimental arrangement used at CETAL (INFLPR) in order to test LIDT is presented below. The LIDT test was conducted on a 25 mm optical flat coated with the thin film of interest. A lens with the focal distance of 410 mm at 800 nm was used to focalise the laser beam. The samples were mounted at 385 mm with respect to the principal plane of the lens to avoid unwanted optical effects, like optical filamentation, that can disturb laser parameters like: spatial profile, pulse duration, spectrum etc.

Laser beam parameters: TEWALAS/INFLPR – max pulse energy: 450 mJ; **Pulse duration**: 25 fs; **Pulse energy**: 5 mJ – 13 mJ (the energy range used for the current test); **Pulse regime**: sigle puls and burst from 2 up to 10 pulses per site; **Repetition rate**: 10 Hz; **CWL**: 800 nm; **Spectral band:** 70 nm. Figure 4 sows the laser beam parameters and figure 5 shows the experimental setup.

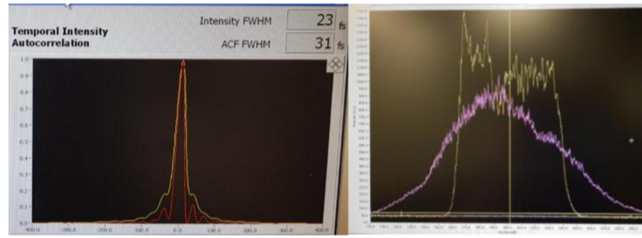

Fig.4 Laser beam parameters (pulse duration and spectrum of the oscillator after the final amplification)

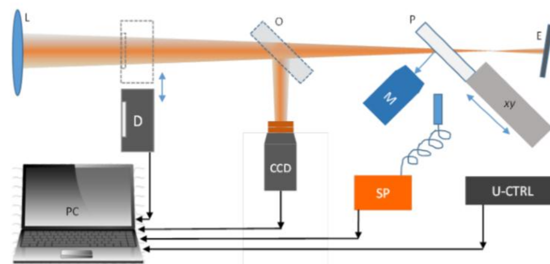

Fig. 5 The outline of the experimental setup for LIDT test

Where: **L** – Focus lens **L** = 410 mm at 800 nm wavelength; **D** – GENTEC energy detector; **O** – mirror for laser profile checking; **CCD** – Ophir laser profilometry camera; **SP** – Thorlabs triggerable spectrometer, model CCS200 / M for laser emission spectrum recording; **M** – DINO microscope; **XY** – motorized translation 50 mm x 50 mm, with STANDA control unit (U-CTRL); **E** – Laser beam lock screen.

Experimental conditions: The laser beam was focused with a 410 mm focal length lens at 800 nm. The beam diameter was 28 mm in the plane of the lens. Before the lens, the beam is diaphragmed to ensure a circular structure of the beam. The samples were placed 25 mm in front of the focal plane of the lens (385 mm compared to the lens), in order to avoid the optical filamentation effects that may appear in focus when focusing in air, so as not to disturb the laser parameters (spectrum, duration of pulse, spatial profile). The normal incidence laser profile is recorded with a BeamGage (Ophir Photonics) CCD camera, placed at a distance from the lens equal to the lens-sample distance.

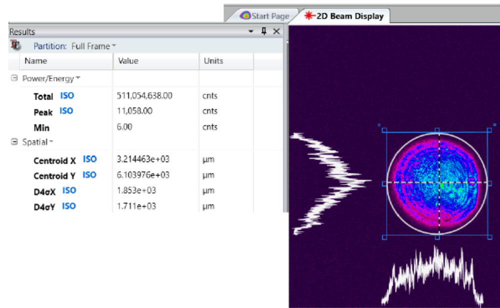

Fig.6 The spatial profile of the laser at 385 mm from the focusing lens, at normal incidence.

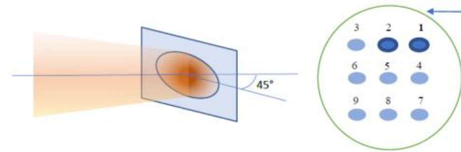

Fig.7 Laser irradiation geometry: 45 ° incidence

Laser irradiation was performed at 45°, with the beam polarized horizontally. In the sample plane, the beams are elliptical due to the angle of incidence. The diameter on the small axis of the ellipse is 1.7 mm. At least 3x3 sites rated with {1,2… 9} with a distance of 10 mm between sites were irradiated. The irradiations for the site no. 1 and the site no. 2 were made under energy conditions and number of pulses where laser ablation is obtained. Thus, the initial position on the sample is always known. When the result for an irradiation was not conclusive, additional irradiation between sites was performed to verify the repeatability, at distances of 0.5 mm as a rule from the initial sites.

Table 3

The results of the single-pulse tests

Sigle pulse	**V1.1**	**V1.2**	**V2.1**	**V2.2**	**V3.1**	**V3.3**	**V4.1**	**V4.2**	**V5.1**	**V5.2**
5 mJ	ok	ok	ok	ok	ok	ok	ok	ok	ok	ok
7 mJ	ok	ok	ok	ok	ok	ok	ok	ok	ok	ok
8.5 mJ	ok	ok		ok	ok	ok	ok	ok	ok	ok
9 mJ	+							++		
10 mJ	+	++	++	++	++	++	+	++	++	++
13 mJ	++	++	++	++	++	++	++	++	++	++

Table 4

Results of burst tests (tests performed up to 10 pulses)

Burst-Pulse damage	**V1.1**	**V1.2**	**V2.1**	**V2.2**	**V3.1**	**V3.3**	**V4.1**	**V4.2**	**V5.1**	**V5.2**
5 mJ (**10 pulsuri**)	ok	ok	ok	ok	ok	ok	ok	ok	ok	ok
7 mJ	ok	ok	+(**2**)	ok	ok	ok	+(1**0**)	ok	ok	ok
8.5 mJ	+ (**10**)	+ (**2**)		++ (**4**)	ok	+ (**4**)		+ (**4**)	+ (**2**)	+ (**10**)
9.5 mJ	++ (**2**)				+ (**2**)					

Where: “ok” - the samples have no damage on the irradiated site; “+” - site with superficial destruction; “++” - site destroyed; (n) - number of pulses recorded.

Figures 8 and 9 illustrates destroyed sites:

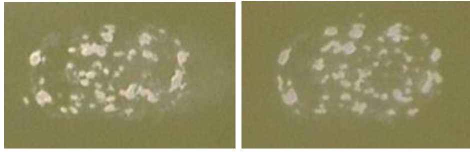

Fig.8 Microscope image for burns typical of sites # 1 and # 2 (13 mJ and 10 mJ)

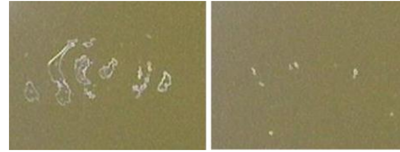

Fig.9 Damage at 8.5 mJ with 4 pulses (left) compared to superficial damage at 8.5 mJ with 2 pulses (right). Test: V1.1.

Laser fluency for optical destruction: The distance of 25 mm between the sample and the focal plane was also chosen to minimize errors in calculating the sample fluency due to imprecise positioning of the sample (± 0.5 mm) or determining the quality factor M^2. An error in calculating the laser fluency below 5% is estimated. Of the same order of magnitude are the energy fluctuations of the laser, from pulse to pulse.

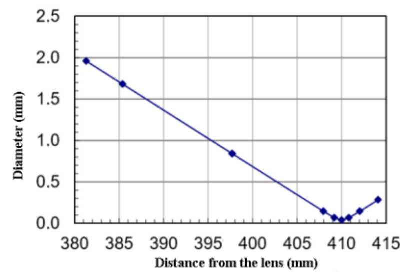

Fig.10 Dependence of the laser spot diameter on the distance to the lens

The formula for calculating laser fluency for a spot with a circular gaussian profile is:

$$F = \frac{2E}{A} \quad (3)$$

and for a top-hat profile it is:

$$F = \frac{E}{A} \quad (4)$$

For the calculation of the laser fluence (mJ/cm^2), the beam diameter of 1.7 mm (25 mm from the focus) was taken into account and a gaussian profile of transverse intensity was considered. The laser quality factor after magnification is $M^2 = 2.5$. However, due to the 25 mm distance between the sample and the focal plane, the quality factor value no longer influences the beam diameter value in the sample plane. For the threshold energy of 7 mJ, the laser fluence value is 0.6 J/cm^2, if normal incidence and Gaussian profile are considered. For the case of a top-hat profile, the calculated fluence value decreases to 0.3 J / cm^2. For incidence

at 45 °, if we take into account the area of the ellipse, the values above will be corrected by a factor of 0.707, respectively 0.43 J/cm^2 for a Gaussian laser profile. Under similar irradiation conditions, a commercial dielectric mirror with reflective coating for 800 nm has been destroyed since the energy of 7 mJ in single-pulse regime. At the same energy all the mirrors tested have withstood.

Fig.11 Site destroyed on a commercial dielectric mirror at 7 mJ energy, single-pulse.

2.5. Another important characteristic of a dispersive optical element is **group delay (GD)**, which is defined as the derivative of the spectral phase with respect to the light frequency ω with a minus sign. **Group delay dispersion (GDD)** is the derivative of GD with respect to ω. It is usually specified in fs^2 or ps^2. Positive (negative) values correspond to normal (anomalous) chromatic dispersion. In order to properly compensate the phase distortion of an optical pulse, special multilayer coatings can be used. These coatings, called dispersive (or chirped) mirrors, provide high reflection and specific GD and GDD wavelength dependencies in required spectral ranges. Modern laser techniques, including femtosecond laser oscillators and external enhancement cavities, require a few fs^2 accuracy of GDD determination that is not achievable with the existing approaches. Most approaches for the measurement of the group-delay dispersion (GDD) of optical elements have been based on a *white-light interferometer* that contains the dispersive element in one arm, keeping the other arm as a reference. The-cross-correlation pattern reveals the wavelength-dependent optical path difference between the two arms [13]. White-light source, used in combination with a standard Michelson interferometer, has been a reliable method for the study of the dispersive properties of optical materials, especially for the femtosecond lasers were the dispersion must be accurately controlled to yield the shortest pulses. An optical element under investigation is placed in the sample arm of the interferometer while the reference arm contains a reference sample with known dispersion. In the course of the measurement process, the reference sample is moved by a motor, and the length of the reference arm is varied. When the reference sample is moved, a spectral intensity distribution (spectral scan) at each motor step position is monitored and recorded. When all scans are recorded, the intensity values can be arranged by the wavelength. A temporal intensity distribution corresponding to a certain wavelength is called an interferogram. GD

at each wavelength can be obtained as an instant corresponding to a center position of the interferogram. An obvious advantage of this measurement scheme is that it enables one to obtain GD simultaneously for all wavelength values generated by a white-light source.

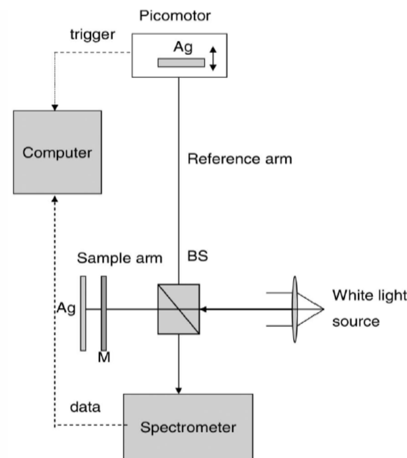

Fig. 12 - Schematic of the white-light interferometer
(where: BS = beam splitter; Ag = silver mirror; M = dispersive mirror under investigation)

Intensity values in measured interferogram are affected by a noise of the light source and by a noise of the detector. Evidently, determination of center positions from noisy interferogram is not a straight forward task. The problem of extracting GD from interferometric measurements has been considered in several works [14, 15]. The most widely used approach is the Fourier transform technique. Results provided by the Fourier transform technique are, however, strongly dependent on the noise in interferometric data. In the case of no uniform motion of a stepper motor, the Fourier transform technique may fail entirely. Correct processing of data requires the application of preliminary smoothing procedures, which significantly decreases wavelength resolution of obtained GD and GDD wavelength dependencies. Figure 12 presents the results for GD and GDD measurement, done on samples of 30 mm diameter that were placed in the same coating batch with the tested mirror:

Measuring system**:** White-light interferometer; GDD resolution: ± 5 fs^2; Wavelength Range: 700.0 nm to 1000.0 nm; 45^0 incident angle.

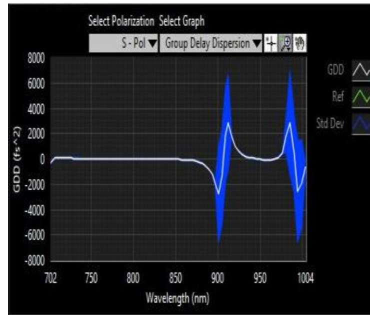

Fig. 13. a- GDD Measurement Results for "S" polarization

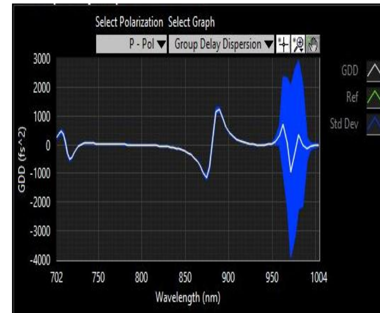

Fig. 13. b- GDD Measurement Results for "P" polarization

As it can be observed in figure 13, in the spectral range of interest [750 850]nm, the value of GDD is obviously less than 50fs^2 while the highest requirements for this parameter have at least a double value (e.g. 100fs^2 for ELI mirrors).

6. Conclusions

This paper presents the results obtained by a team that had as main goal to design, manufacture and test a large mirror (150mm diameter) used for transporting of a high energy, femtosecond laser beam on the spectral range [750 850] nm. After describing the particularities of this propose, the testing arrangements, methods and results obtained were presented. In a short recap, the testing results were as follows: **Flatness**, around λ/19; **Roughness**, less than 2nm; **Average Reflectance**, higher than 98%; **Group Delay Dispersion** (GDD), lower than 50fs^2 and, the most important parameter **Laser Induced damage Threshold (LIDT)**, having the following data results, relative to the pulse energy:

- at 5 mJ in single-pulse regime, all the sites at all the samples have resisted.
- at 7 mJ in single-pulse regime, all the sites at all the samples have resisted.
- at 5 mJ in burst mode 10 pulses, all the sites at all the samples have resisted.
- at 10 mJ in single-pulse regime all sites at all samples were destroyed.

Differentiation between samples is made at energies of about 7-8 mJ, for 1 laser pulse up to 10 pulses (at 10 Hz frequency). The threshold energy of destruction is estimated to be around 0.4 J/cm2. For a more precise determination of the destruction threshold, the standard s-on-1 method must be applied [9]. In this regard, the TEWALAS facility is under upgrade procedure and the tests results will be published in the next paper that will be exclusive dedicated to this method, experimental arrangement and obtained results.

REFERENCES

[1]. *Roxana Damian, A. Rizea, C. Cotirlan-Simioniuc, Cristina Gheorghiu, A. Naziru, M. Georgescu,* "Processing of large laser grade mirror substrates", U.P.B. Sci. Bull., Series D, Vol. 81, Iss. 4, 2019

[2]. The White Book of ELI Nuclear Physics Bucharest-Magurele, Romania

[3]. *M.I Kaganov, I.M Lifshitz,* and *L.V. Tanatarov,* "Relaxation between Electrons and Lattice", J. Exp. Theor. Phys. 31(2): pp. 232-237 ,1956

[4]. *C. B. Schaffer,* "Interaction of Femtosecond Laser Pulses with Transparent Materials", PhD thesis, Harward University, 2001

[5]. Infomatik-N Software Manual for Phase Interferometer V-100/P, 2004

[6]. *Michael Bass, Eric W. Van Stryland, David R. Williams, William L. Wolfe*, "Handbook of optics - Fundamentals, Techniques, and Design", vol. I, 2nd Edition, Sponsored by the Optical Society of America, 1995

[7].https://www.bruker.com/products/surface-and-dimensional-analysis/atomic-force microscopes/modes/modes/imaging-modes/tapping-mode.html

[8]. https://www.slideshare.net/joybiitk/atomic-force-microscope-fundamental-principles

[9]. *R. Stoian, D. Ashkenasi, A. Rosenfeld*, and *E. E. B. Campbell*, "Coulomb explosion in ultrashort pulsed laser ablation of Al_2O_3" Physical Review B, vol. 62, no. 19, pp. 13167–13173, 2000;

[10]. *B. Rethfeld, V. V. Temnov, K. Sokolowski-Tinten, P. Tsu, D. von der Linde, S. I. Anisimov, S. I. Ashitkov, and M. B. Agranat,* "Superfast thermal melting of solids under the action of femtosecond laser pulses", J. Opt. Technol., vol. 71, no. 6, pp. 348–352, 2004;

[11]. ISO 21254: Optics and optical instruments. Lasers and laser related equipment. Test methods for laser induced damage threshold of optical surfaces. Part 1: 1 on 1-test, 2000, part 2: S on 1 test, 2001, part 3: Assurance of laser power handling capabilities 2011, International Organization of Standardization ,2011;

[12]. *A. Zorila, A. Stratan* and *G. Nemes*, "Comparing the ISO-recommended and the cumulative data-reduction algorithms in S-on-1 laser damage test by a reverse approach method", Review of Scientific Instruments 89, 013104, 2018;

[13]. *Tayyab Imran, Kyung-Han Hong, Tae Jun Yu, Chang Hee Nam*, "Measurement of the group-delay dispersion of optical elements using white-light interferometry", Review of Scientific Instruments, vol. 75, no. 7, 2004;

[14]. *W. H. Knox, N. M. Pearson, K. D. Li, and C. A. Hirlimann*, "Interferometric measurements of femtosecond group delay in optical components", Opt. Lett. 13, pp. 574–576, 1988

[15]. *W. H. Knox*, "Dispersion measurements for femtosecond-pulse generation and applications", Appl. Phys. B 58, pp. 225– 235, 1994.